Journal of Applied Electrochemistry **33**: 457–463, 2003.
© 2003 *Kluwer Academic Publishers. Printed in the Netherlands.*

Electrochemical investigations on the influence of electrolyte composition of Watts baths with special regard to throwing power

S. WEHNER[1], A. BUND[1], U. LICHTENSTEIN[1], W. PLIETH[1,*], W. DAHMS[2] and W. RICHTERING[2]
[1]*Dresden University of Technology, Institute of Physical Chemistry and Electrochemistry, Mommsenstrasse 13, D-01062 Dresden, Germany*
[2]*Atotech Germany GmbH, Erasmusstrasse 20, D-10553 Berlin, Germany*
*(*author for correspondence, fax: +49 (0)351 463 37164, e-mail: waldfried.plieth@chemie.tu-dresden.de)*

Received 10 June 2002; accepted in revised form 21 February 2003

Key words: activation energy, nickel electroplating, quartz crystal microbalance, throwing power, Watts bath

Abstract

The influence of a variety of substances on technically relevant parameters of a nickel electroplating electrolyte (Watts bath) has been investigated. Special attention has been paid to the throwing power (TP), as well as visual appearance, current efficiency and codeposition of foreign atoms. Systems reported in the literature (e.g., inorganic salts to increase conductivity or complexing agents to increase polarization) were compared with typical reducing agents normally used in electroless Ni deposition. The mechanism of TP improvement in the case of sodium hypophosphite and dimethylamine-borane has been examined with the electrochemical quartz crystal microbalance (EQCM). Using the EQCM it was shown that there is a synergistic effect between the electrochemical and electroless deposition process. In addition, the activation energy of the latter was determined from temperature dependent measurements.

List of symbols

A	area
C	proportionality factor in the kinetic equation, describing the temperature dependence of the electroless plating rate
C_{SB}	Sauerbrey constant
E_A	activation energy
i	current density
k	Wagner parameter
L	distance ratio in the Haring–Blum cell
m	mass
M	mass ratio in the Haring–Blum cell
R	gas constant
T	absolute temperature
U	electric potential
t	time
Δf	frequency shift
κ	electrolytic conductivity

1. Introduction

Electrochemical nickel plating is a widely used process. Applications comprise functional coatings, for example, for corrosion protection, increase of wear resistance and decorative coatings such as bright Ni mostly in combination with chromium. Many electrolyte formulations are based on the classical composition proposed by Watts, which yields dull Ni deposits. To obtain decorative deposits with a mirror-like surface finish special additive formulations have been developed, which contain organic substances like surfactants, brighteners and levellers. The current efficiency is nearly 100% over a wide range of current densities. However, it is difficult to obtain a uniform deposition thickness distribution on complex shaped substrates, as a consequence of the nonuniform current density distribution. For the majority of applications a uniform thickness distribution on irregularly shaped substrates is desired, which requires an electrolyte with good throwing power (TP).

Empirical investigations have shown that the TP increases with cathodic polarization and with electrolyte conductivity [1]. These two quantities have been summarized in a theoretical treatment by Wagner (Wagner parameter k, Equation 1) [1, 2]:

$$k = \kappa\left(\frac{\mathrm{d}U}{\mathrm{d}i}\right) \tag{1}$$

The Wagner parameter, k, which should be proportional to the TP, increases with increasing electrolyte conductivity κ and the slope of the polarization curve ($\mathrm{d}U/\mathrm{d}i$) under steady conditions.

In the electroplating industry an assessment of the TP is done by determining the thickness of the plating on a cathode, or several electrically connected cathodes, as a function of the distance from the anode. The

Haring–Blum cell or the Hull cell are widely used experimental set-ups. The percentage TP can be calculated with the relation given by Field (Equation 2):

$$\mathrm{TP} = \frac{L - M}{L + M - 2} \times 100 \quad (2)$$

where L is the ratio of the distances of the cathodes from the anode, and M is the ratio of the deposited masses. Usually a distance ratio of 5:1 for the cathodes is used. The determination of TP is described in [3, 4].

Recently, it has been found that the TP of a Watts electrolyte is increased by adding sodium hypophosphite [5]. Hypophosphite is used in electroless Ni deposition, because it acts as a reducing agent for Ni ions. Therefore, an investigation was carried out to examine the relation between an increase in TP and the reducing properties and to analyse the individual contributions of the electrochemical and the electroless deposition processes. The electrochemical quartz crystal microbalance (EQCM) proved to be a valuable tool for these investigations. Frequency shifts of a quartz crystal are related to changes in the areal mass density at its surface by the Sauerbrey relation (Equation 3) [6]:

$$\Delta f = -C_{\mathrm{SB}}\left(\frac{m}{A}\right) \quad (3)$$

where Δf is the shift of the resonance frequency of the quartz crystal, m/A the areal mass density, and C_{SB} the Sauerbrey constant (226.014 Hz cm^2 μg^{-1} for a 10 MHz quartz, see Section 2).

Besides the effect of hypophosphite, the influence of sulphur-, boron- and phosphorus-containing reducing agents and some organic substances was studied, some of which have been proposed as possible candidates to improve the TP. Another aim of the work was to investigate how these substances influence the visual appearance of the deposits, the codeposition of foreign atoms and the current efficiency.

2. Experimental details

The electrolytes examined were based on a typical Watts bath, containing 0.17 M $NiSO_4 \cdot 6H_2O$, 0.77 M $NiCl_2 \cdot 6H_2O$ (both purity 98%, Grüssing GmbH, Germany), 0.65 M H_3BO_3 (99.5%, Riedel de Haen). The pH value was adjusted to 4.2 ± 0.2 with 1 M $NaHCO_3$ or 2 M H_2SO_4. An electrolyte for bright Ni deposition was obtained by adding a commercial additive formulation (Duplalux G, wetting agent Ni 719 and a 'brightness correction solution Ni', Atotech, Berlin, Germany) to this electrolyte. Table 1 lists the investigated substances together with their concentration ranges in the electrolytes (Watts or bright Ni electrolyte). Highly purified water was used for the preparation of all solutions.

Polarization curves for the determination of the Wagner parameter (Equation 1) were measured using an EG&G 263A potentiostat (PAR, Oak Ridge, USA) in a thermostated glass cell (55 ± 1 °C). The working electrode was a rotating (500 rpm) Ni disc of 0.28 cm^2 surface area. A saturated calomel electrode (SCE) was used as reference electrode and a Ni sheet as counter electrode. All potentials are quoted with reference to the SCE. The electrolytes were purged with nitrogen at least 10 min prior to the experiment. The conductivity of the electrolytes was measured at room temperature with a conductivity meter.

The substrates for the galvanostatic depositions were degreased with CH_2Cl_2, activated in 1 M HCl + 2 M H_2SO_4, rinsed with deionized water, immersed in 2 M H_2SO_4, and thoroughly rinsed again. The determination of the TP followed the procedure by Haring and Blum [7] in a double jacketed cell (made in-house, poly(eth-

Table 1. Investigated substances, concentration range and their effect on the Wagner parameter and the TP

Substance	c /mol l^{-1}	Wagner parameter*	TP*	Remarks
Citric acid ($C_3H_4(OH)(COOH)_3$) Bright Ni electrolyte	0.100–0.800	++	++	h.c.d.: white blooming
Tartaric acid ($C_4H_2(OH)_4O_2$) Bright Ni electrolyte	0.029–0.095	−−	+	
Mannite ($C_6H_8(OH)_6$) Bright Ni electrolyte	0.082–0.330	−	0	
Sodium dithionite ($Na_2S_2O_4$)	decomposition in the electrolyte during the deposition fine-grained black precipitation			
Potassium disulfite ($K_2S_2O_5$) alone or with 0.040 M $MgSO_4$	0.002–0.045	−−	−−	h.c.d.: black loose deposits
Watts electrolyte, Bright Ni electrolyte				l.c.d.: black bloomy coating
Sodium hypophosphite (NaH_2PO_2) Watts electrolyte	0.047–0.189	0	++	
Sodium phosphite (Na_2HPO_3) Bright Ni electrolyte, Watts electrolyte	0.005–0.100	not detd.	0	
Dimethylamine-borane (DMAB) $(CH_3)_2NHBH_3$ Bright Ni electrolyte	0.017–0.160	not detd.	++	non-uniform visual appearance

* Code: (++) increase, (+) slight increase, (0) no effect, (−) slight decrease, and (−−) decrease with increasing concentration of the corresponding substance.

ylene), 12.2 cm × 2.9 cm × 5.1 cm). Ni was deposited from an unstirred electrolyte at 2 A dm^{-2} for 1800 s at 55 ± 3 °C on two Cu substrates (each 12.5 cm^2) with a distance ratio of 5:1 relating to a perforated Ni anode. The mass of the deposited Ni was determined by weighing the substrate before and after deposition. The TP was calculated from Equation 2.

To investigate the visual appearance over a wide current range and the average current efficiency Ni depositions (55 ± 3 °C, 2.5 A for 600 s) on Cu substrates precoated with a Ni strike were performed. The Ni strike (1 M $NiCl_2 \cdot 6H_2O$, 1 M HCl, 4–8 A dm^{-2}, 120 s, room temperature, Ni anode) was applied to rule out effects from the base material. The electrolyte was stirred with an electrically driven paddle (about 45 oscillations per minute) to mimic industrial plating conditions. A Ni sheet was used as anode.

Scanning electron microscopy (SEM) and energy dispersive X-ray analysis (EDX) investigations were performed with a Zeiss DSM 982 Gemini microscope (Carl Zeiss, Germany). As no special calibration procedure was performed, the error of the EDX measurements is about 5%.

In the following, the part of the Hull cell substrate (cathode) with a short distance to the anode is called the high current density (h.c.d.) edge, the long distance part is called the low current density (l.c.d.) edge.

Electrochemical quartz crystal microbalance (EQCM) experiments were carried out in a double jacketed glass cell. The working electrode was one side of a quartz crystal (AT cut, 10 MHz with Au electrodes on a Cr adhesion layer), supplied by KVG (Neckarbischofsheim, Germany). Details concerning the measuring technique can be found elsewhere [8].

3. Results and discussion

3.1. *Throwing power, visual appearance, codeposition of foreign atoms and current efficiencies*

3.1.1. *Citric acid, tartaric acid, mannite*

No increased codeposition of foreign atoms (e.g., C, O) was detected in the presence of citric acid, tartaric acid and mannite. For all substances SEM examination showed fine-grained homogeneous deposits over the entire current density range and in the concentration range investigated.

Due to complexation of the Ni ions the deposition potential of Ni shifted to more cathodic values with increasing concentration of citric acid [9]. This finding corresponds to an increased polarization, and according to the Wagner parameter an enhanced TP could be expected [1]. In the concentration range 0.4–0.8 M, the citric acid enhanced the TP (Figure 1). The current efficiency decreased with increasing concentration of citric acid, e.g. to about 65% at equimolar ratio of Ni and citric acid. At current densities above 3 A dm^{-2} the surface of the deposit had a white foggy appearance,

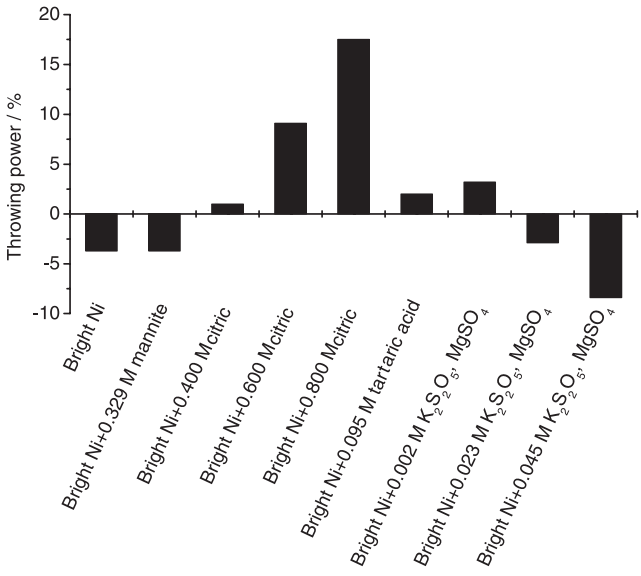

Fig. 1. Throwing power (according to Fields, Equation 2) of bright Ni electrolyte with different substances.

which became more pronounced at higher concentrations.

As tartaric acid should also form complexes with Ni ions, similar effects as in the case of citric acid were expected. However, the Wagner parameter did not change significantly in the presence of tartaric acid. Compared to citric acid, the insignificant effect of tartaric acid may be caused by its lower concentration (Figure 1). Besides a green precipitate at the h.c.d. edge, the visual appearance and the current efficiency showed no substantial changes compared to the pure electrolyte.

In the case of mannite the Wagner parameter did not change significantly, and experiments in the Haring–Blum cell showed a slight increase of the TP (Figure 1). The deposits had the same visual appearances as those from the pure electrolyte.

3.1.2. *Potassium disulfite ($K_2S_2O_5$)*

Potassium disulfite ($K_2S_2O_5$) spontaneously decomposes to sulfurous acid in aqueous solutions (Equation 4).

$$S_2O_5^{2-} + H_2O \rightleftharpoons 2\,HSO_3^- \qquad (4)$$

It has been reported, that the TP of a Watts electrolyte is increased in the presence of $K_2S_2O_5$ alone or together with $MgSO_4$ [10]. As Reaction 4 proceeds quantitatively, the anion HSO_3^- should be responsible for the increase of the TP. In the experiments discussed here slight decreases of both the Wagner parameter and the TP were observed (Figure 1). The obtained coatings showed a black nonadherent layer at the h.c.d. edge and a gray cover at the l.c.d. edge with increasing concentration. At the anode a black film formed, which was soluble in sulfuric acid. At concentrations above 0.023 M $K_2S_2O_5$ a black precipitate formed in the electrolyte. The amount of codeposited S increased with increasing concentration.

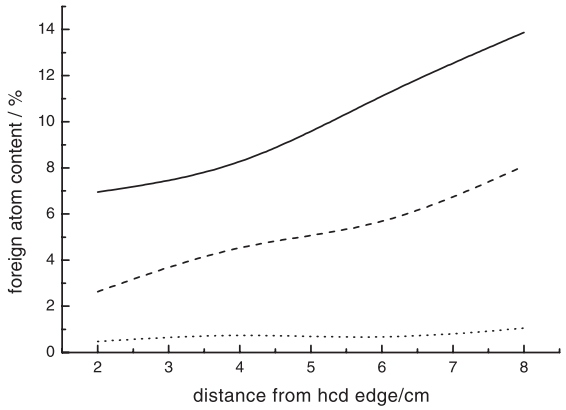

Fig. 2. Codeposition of foreign atoms. Watts electrolyte with 0.094 M sodium hypophosphite (——), bright Ni electrolyte with 0.023 M potassium disulfite and 0.040 M $MgSO_4$ (– – –), bright Ni electrolyte with 0.002 M potassium disulfite (···).

In agreement with [11] it was found, that the amount of sulphur was higher at the l.c.d. edge (Figure 2, dashed line and dotted line).

SEM examination showed a fine-grained homogeneous metal deposition in the l.c.d range and an inhomogeneous film with a blistered structure in the h.c.d range (Figure 3). The formation of cracks and the bad adherence of the layers in the h.c.d range increased with increasing concentration of $S_2O_5^{2-}$. Therefore, a detailed analysis of the current efficiencies was not possible.

3.1.3. *Sodium dithionite ($Na_2S_2O_4$)*

During the plating from electrolytes with $Na_2S_2O_4$ a black fine-grained precipitation was generated at the anode and in the electrolyte. Probably, this was caused by the decomposition of $Na_2S_2O_4$ in aqueous media (Equation 5) [12] and the formation of insoluble products from the decomposition products themselves or their oxidation products.

$$2\,S_2O_4^{2-} + H_2O \rightleftharpoons 2\,HSO_3^- + S_2O_3^{2-} \qquad (5)$$

Reaction 5 shifts to the right under the deposition conditions (high temperature). Due to the bad quality of the deposits (inclusion of the precipitate) no investigations of Wagner parameter, foreign atom codeposition and current efficiencies were carried out. As the anion $S_2O_4^{2-}$ decomposes to HSO_3^- and $S_2O_3^-$ (Equation 5), neither of these species seems to improve the TP (see also results with $K_2S_2O_5$).

3.1.4. *Sodium hypophosphite (NaH_2PO_2, SHP)*

The TP of Watts and bright Ni electrolytes increased in the presence of SHP (Figure 4). The effect was stronger for the Watts electrolyte than for the bright Ni electrolyte (not shown). Furthermore, the coatings from the Watts electrolyte had a more homogeneous visual appearance than those from the bright Ni electrolyte. These findings can be explained by the competitive adsorption between the additives (brighteners) and the hypophosphite anion [13].

In the entire current density range a dull coating occurred and only at the h.c.d. edge was a powdery

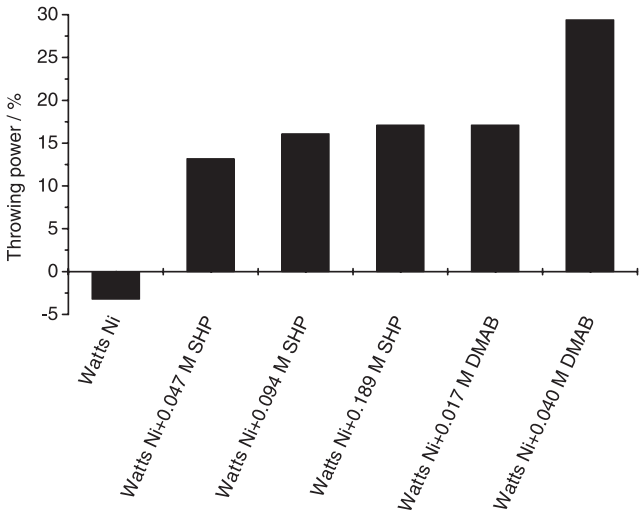

Fig. 4. Throwing power (according to Fields, Equation 2) of Watts electrolyte with different reducing agents.

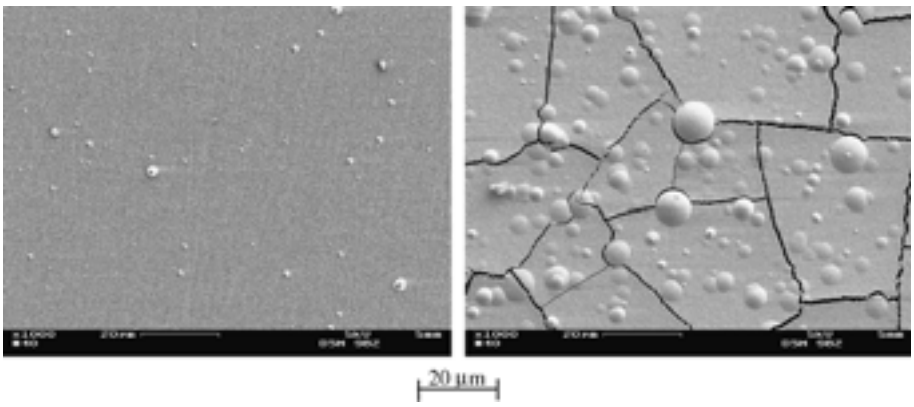

Fig. 3. Scanning electron micrographs of the deposit from bright Ni electrolyte with 0.050 M potassium disulfite Left: l.c.d. range, right: h.c.d. range.

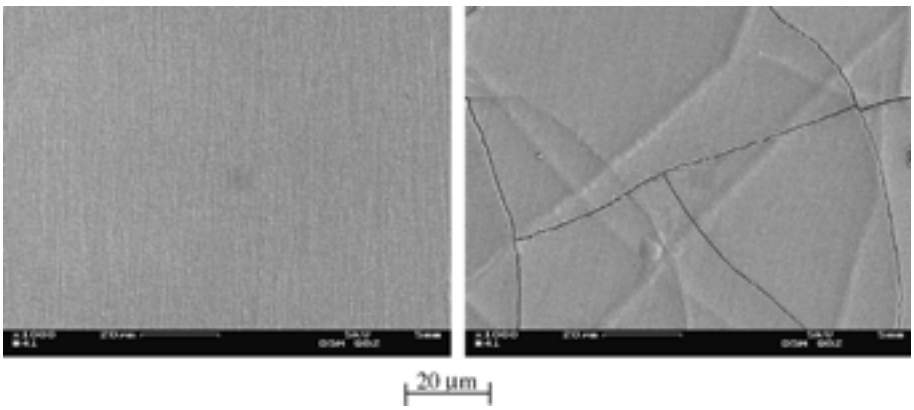

Fig. 5. Scanning electron micrographs of the deposit from Watts electrolyte with 0.142 M SHP. Left: l.c.d. range, right: h.c.d. range.

deposit generated. When the concentration of SHP and the deposition time were small, the described effect was less pronounced. Possibly, the electrochemical oxidation of the reducing agent caused the formation of phosphate [14], which is known to produce rough and loose coatings at high concentrations [15].

EDX investigations indicated an increased P inclusion with increasing SHP concentration. As in the case of S inclusion, this effect was strongest in the l.c.d range (Figure 2). A fine-grained homogeneous layer in all current density ranges was observed by SEM (Figure 5). Fissuring occurred in the h.c.d range because of increasing internal stress with decreasing P content [16]. The effect was less pronounced than in the case of S (Figure 3).

The improvement of the TP is not predicted by the Wagner parameter, which decreased with increased concentration of SHP (Table 1). This behaviour is probably caused by the overlapping of the partial cathodic currents, that is, the reduction of Ni^{2+} and $H_2PO_2^-$, respectively. Obviously, the sum of the currents produced a decreased slope (dU/di) with increased SHP concentration. The higher conductivity of the SHP electrolyte was overcompensated by the decrease of (dU/di). The current efficiency amounted to about 100% in the investigated concentration range.

3.1.5. *Sodium phosphite (NaH_2PO_3)*
In the bright Ni electrolyte gray films were formed. As in the case of SHP (Section 3.1.3) this might be caused by the competition of phosphite anions and the organic components. In the Watts electrolyte a dull coating was obtained at medium current densities.

3.1.6. *Dimethylamine-borane (DMAB, $(CH_3)_2NHBH_3$)*
Besides SHP dimethylamine-borane is utilized as a reducing agent for electroless deposition [17]. The increase of the TP with increasing DMAB concentration occurred in the same order of magnitude as in the case of SHP. The visual appearance was grey and foggy with increased DMAB concentration at medium and high current densities. A white coat formed in the l.c.d ranges. Furthermore, a powdery precipitation occurred at the outer h.c.d edge. Another disadvantage is the formation of Ni on the cell walls after longer periods by autocatalytic Ni deposition. In contrast to S and P containing substances, fissuring was observed in the l.c.d range. This effect increased with increasing DMAB concentration. The current efficiency remained at about 100% over the DMAB concentration range investigated. The Wagner parameter was not determined, because of the inadequately reproducible $U(i)$ curves.

3.2. *Temperature dependence of electroless Ni deposition*

The reducing agents SHP and DMAB showed the best improvement of the TP (Sections 3.1.4 and 3.1.6 and Figure 4) which could be caused by an overlapping of electroless and electrochemical deposition. To separate the two contributions EQCM analyses were performed.

As a first result, it was observed, that no mass increase occurred at the native gold electrode of the EQCM in Ni electrolytes with SHP or DMAB. The necessity of an activating procedure is reported in [18, 19]. In [20, 21] it was claimed that the Au oxide surface layer had to be reduced before electroless Au deposition with DMAB could occur. In the present case a continuous Ni deposition could only be obtained after a cathodic potential of at least −0.8 V had been applied. Because this activation potential is slightly cathodic to the bulk Ni reduction (about −0.7 V), the formation of Ni nuclei seems to be the crucial activation process in the case of electroless Ni deposition.

The critical areal mass density of Ni nuclei below which no electroless Ni deposition occurred was about 5 $\mu g\ cm^{-2}$ in the case of the bright Ni electrolyte with 0.034 M DMAB at 313 K. Above this coverage which quantitatively agrees with literature [22] a continuous mass increase set in.

Another interesting feature of the activation process is illustrated in Figure 6. After 10 s of activation at −0.9 V the mass on the quartz increased by electroless deposition within 120 s to 1.8 $\mu g\ cm^{-2}$ (circles). Activation for 30 s at the same potential produced a six times larger mass of nuclei, which in turn gave rise to a stronger electroless deposition, 6.8 $\mu g\ cm^{-2}$ in 120 s (up triangles).

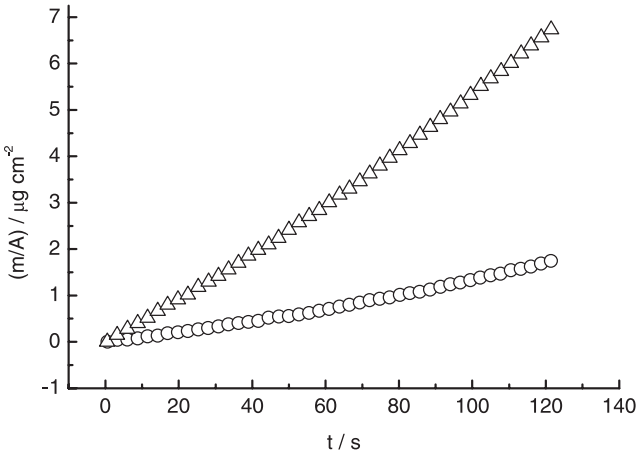

Fig. 6. Mass increase indicated by the EQCM by electroless Ni deposition from a bright Ni electrolyte with 0.034 M DMAB after activation at −0.9 V for 10 s (○) and 30 s (△).

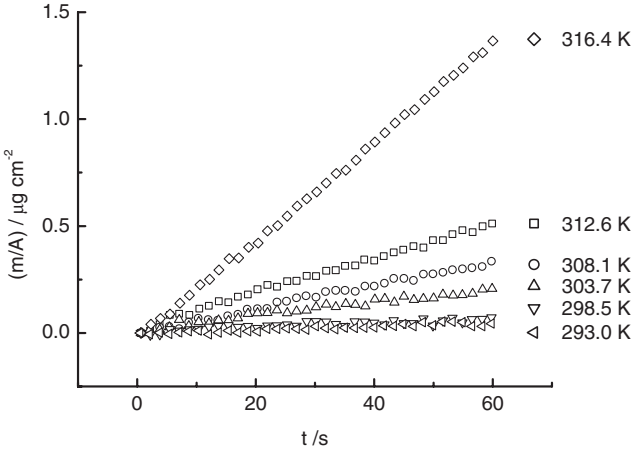

Fig. 7. Temperature dependence (20–43 °C) of the mass increase by electroless Ni deposition from bright Ni electrolyte with 0.034 M DMAB. Activation of the gold electrode surface at −1.0 V for 10 s.

A mass ratio of 1:6 for the nuclei resulted in a mass ratio for the electroless Ni of about 1:4, which indicates, that there seems to be a limiting number of catalytic nuclei, above which no further increase of the electroless deposition rate is observed.

For all further experiments the surface of the Au electrode was activated with 10–20 μg cm^{-2} Ni nuclei, deposited at −1.0 V.

The rate of the electroless Ni deposition strongly depends on temperature [23]. To determine the deposition rate at 55 °C and to estimate its error, a series of measurements at increasing temperatures was performed. It was assumed, that the deposition rate per unit area $(1/A)(\mathrm{d}m/\mathrm{d}t)$ is controlled by an activation energy E_A and can be described by an Arrhenius expression (Equation 6):

$$\frac{1}{A}\left(\frac{\mathrm{d}m}{\mathrm{d}t}\right) = C\exp\left(-\frac{E_A}{RT}\right) \tag{6}$$

where A is the mass sensitive area, C the proportionality factor (depending on the electrolyte composition), T the absolute temperature, and R the universal gas constant (8.314 J mol^{-1} K^{-1}). A logarithmic plot of Equation 6 against $(1/T)$ should give a straight line with a slope of $-E_A/R$.

In the bright Ni electrolyte with 0.034 M DMAB the electroless Ni deposition increased with temperature (Figure 7). The activation energy (Table 2) was determined from an Arrhenius plot (Figure 8) to 128 ± 10 kJ mol^{-1}. This value is higher than reported values (35–64 kJ mol^{-1}) [24 and references therein], which can be explained by the different electrolyte compositions [24].

In the same way, the activation energy of the electroless Ni deposition from a Watts electrolyte with 0.094 M SHP was determined to 44 ± 6 kJ mol^{-1} (Table 2, Figure 8), which is in the same order of magnitude as values reported in literature for different electrolytes, 46–96 kJ mol^{-1} [24, 25].

3.3. *Contribution of the electroless deposition to the total Ni deposition rate*

The rate of the electroless Ni deposition at 55 °C, as well as an error estimate, can be obtained from Equation 6, using the results of the linear regression analysis (Table 2): in a Watts electrolyte with 0.094 M SHP and in a bright Ni electrolyte with 0.034 M DMAB they amount to (0.24 ± 0.05) μm h^{-1} and (0.46 ± 0.08) μm h^{-1}, respectively. If one assumes, that the total deposited thickness is the sum of an electroless and an electrochemical contribution and deducts the electroless contribution from the total thickness (as determined in the Haring–Blum cell), an increase of the TP between 1 and 2% results.

Therefore, at first glance the influence of the electroless plating seems to play a minor role. A significant influence on the TP would result at deposition rates, which are typical for commercial electroless Ni electrolytes, about 10–25 μm h^{-1}. They work with relative low Ni concentration, high temperatures (usually 90 °C), complexing agents, stabilizers, promoters, etc. This explains the relatively small electroless deposition rates

Table 2. Kinetic data (Equation 6) for the electroless Ni deposition from a Watts and a bright Ni electrolyte with SHP and DMAB

Reducing agent and electrolyte	ln C /g cm^{-2} s^{-1}	E_A /kJ mol^{-1}	Deposition rate at 55 °C /μm h^{-1}
0.094 M SHP, Watts	−0.7 ± 2.0	43 ± 6	0.24 ± 0.05
0.034 M DMAB, bright Ni	31.0 ± 3.8	128 ± 10	0.46 ± 0.08

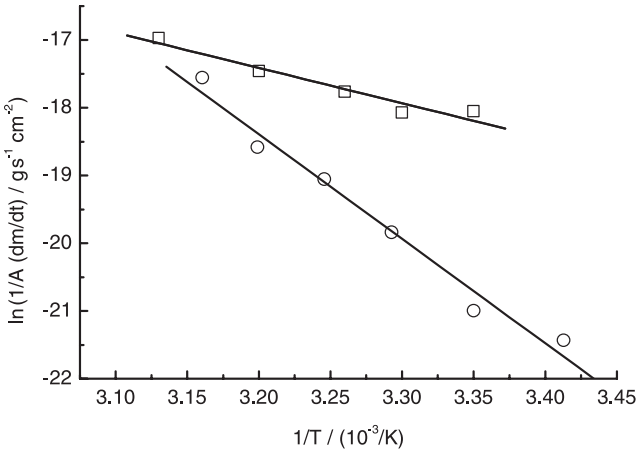

Fig. 8. Determination of the activation energy of electroless Ni deposition from an Arrhenius plot. (□) Watts electrolyte with 0.094 M SHP, (○) bright Ni electrolyte with 0.034 M DMAB, (——) regression lines.

in our case (Table 2). To explain the improvement of the TP by SHP and DMAB a synergistic effect, which varies with the local current density, must be assumed. In the case of electroless deposition of Ni–P alloy an increase in deposition rate was found if a small cathodic current was applied [22], due to a synergistic effect by the continuous generation of Ni nuclei, which should stimulate the electroless process. In the case discussed here smaller Ni nuclei with higher catalytic activity are formed at places of lower current density. As a consequence the inhomogeneous current distribution is transformed into a uniform metal distribution (i.e., an increased TP).

4. Summary

In the electrolytes investigated the TP decreases in the following order: DMAB > sodium hypophosphite > citrate > tartaric acid > mannite > potassium disulfite. For some of the investigated systems a correlation of the Wagner parameter and the TP was observed. A disagreement was found in the case of SHP in Watts electrolyte, which is probably caused by an overlapping of reduction currents of the different electroactive species. The two most promising candidates, DMAB and SHP, led to homogeneous but dull coatings. Therefore, to obtain bright Ni deposits with high TP some optimizations of the electrolyte composition are still necessary. The mechanism of the TP improvement by the reducing agents cannot be explained by a simple overlapping of the electroless and electrochemical reaction, a synergistic effect seems to be active.

Acknowledgement

Financial support from the 'Fonds der Chemischen Industrie' is gratefully acknowledged.

References

1. K. Müller and E. Raub, *Metalloberfläche* **15** (1961) 262.
2. H.W. Dettner and J. Elze, 'Handbuch der Galvanotechnik', Bd 1/II (Carl Hanser Verlag, München, 1966), p. 147.
3. T.C. Tan, *J. Electrochem. Soc.* **134** (1987) 3011.
4. T.C. Tan, *Plat. Surf. Finish.* **74** (1987) 67.
5. Z. Abdel-Hamid, *Mater. Chem. Phys.* **53** (1998) 235.
6. G. Sauerbrey, *Z. Phys.* **178** (1964) 457.
7. H.E. Haring and W. Blum, *Trans. Am. Electrochem. Soc.* **44** (1923) 313.
8. A. Bund and G. Schwitzgebel, *Electrochim. Acta* **45** (2000) 3703.
9. A. von Krusenstjern and E. Raub, *Metall* **14** (1960) 521.
10. S. John, M. Selvam, N.V. Shanmugam and K.N. Srinivasan, *Met. Finish.* **90** (1992) 48.
11. R. Brugger, 'Die Galvanische Vernicklung', 2nd edn. (Eugen G. Leuze Verlag, Saulgau/Württ., Germany, 1984) p. 60.
12. A.F. Holleman, E. Wiberg, 'Lehrbuch der Anorganischen Chemie', 101th edn., (de Gruyter, Berlin, New York, 1995).
13. L.M. Abrantes, M.C. Oliveira, J.P. Bellier and J. Lecoeur, *Electrochim. Acta* **39** (1994) 1915.
14. L.M. Abrantes, A. Bewick, J.P. Correia, M.C. Oliveira and M. Kalaji, *J. Chem. Soc., Faraday Trans.* **93** (1997) 115.
15. 'Inco Taschenbuch der Vernicklung', 3rd edn. (Inco Ltd., 1989).
16. F.A. Lowenheim, Electroplating, Technical Reference Publications Ltd., Port Erin, 1995.
17. M. Schlesinger and M. Paunovic (Eds), 'Modern Electroplating', 4th edn., (Electrochemical Society, Pennington, NJ, 2000).
18. W. Riedel, 'Funktionelle chemische Vernicklung' (Eugen G. Leuze Verlag, Saulgau/Wüertt., Germay, 1989).
19. K. Stallmann, *Galvanotechnik* **75** (1984) 1251.
20. A. Sargent, O.A. Sadik and L.J. Matienzo, *J. Electrochem. Soc.* **148** (2001) C257.
21. A. Sargent and O.A. Sadik, *J. Electrochem. Soc.* **148** (2001) C413.
22. R. Stevanovic, J. Stevanovic and A. Despic, *J. Appl. Electrochem.* **31** (2001) 855.
23. W. Dahms and R. Schumacher, *Galvanotechnik* **87** (1996) 3963.
24. I. Ohno, S. Haruyama and O. Wakabayashi, *J. Electrochem. Soc.* **132** (1985) 2323.
25. P. Cavallotti and G. Salvago, *in* L.T. Romankiw and R. Turner (Eds), Proceedings of the Symposium on Electrodeposition Technology, Theory and Practice', **PV 87-17**, (Electrochemical Society, Pennington, NJ, 1987), p. 327.